Rare Metal Materials and Engineering
Volume 51, Issue 3, March 2022
Available online at www.rmme.ac.cn

Science Press

Cite this article as: Zhao Zhenduo, Li Sha, Xu Mei, et al. Constitutive Model Based on Dislocation Density Theory for Nuclear-Grade 316LN Stainless Steel at Elevated Temperatures[J]. Rare Metal Materials and Engineering, 2022, 51(03): 888-894.

ARTICLE

Constitutive Model Based on Dislocation Density Theory for Nuclear-Grade 316LN Stainless Steel at Elevated Temperatures

Zhao Zhenduo[1], Li Sha[1], Xu Mei[1], Pei Haixiang[2], Fan Guangwei[1], Zhao Zilong[3]

[1] State Key Laboratory of Advanced Stainless Steel, Taiyuan Iron & Steel (Group) Co., Ltd, Taiyuan 030003, China; [2] School of Materials Science and Engineering, North University of China, Taiyuan 030051, China; [3] School of Chemical Engineering and Technology, Sun Yat-sen University, Zhuhai 519082, China

Abstract: The compression deformation behavior of 316LN austenitic stainless steel was investigated at 1050~1200 °C under strain rate of 0.1, 1, 50 s^{-1}. The influence of deformation temperature and strain rate on the hot flow curves was analyzed. Based on the dislocation density theory, the hot deformation constitutive model of 316LN steel was established. The softening mechanism of the 316LN steel was revealed. The results show that the dynamic recrystallization (DRX) dominates the softening mechanism under the condition of high temperature and low strain rate (<0.1 s^{-1}); the dynamic recovery (DRV) dominates the softening mechanism under the condition of high temperature and high strain rate (>1 s^{-1}); DRX and DRV dominate the softening mechanism under the condition of high temperature and strain rate of 0.1, 1 s^{-1}. The established constitutive model can precisely predict the hot deformation behavior of 316LN steel: its Pearson correlation coefficient is 0.9956 and the average absolute value of relative error is 3.07%, indicating the accuracy of this constitutive model.

Key words: austenitic stainless steel; constitutive model; dislocation density; softening mechanism; critical strain; hot deformation; work hardening

316LN austenitic stainless steel is widely used in main pipeline for nuclear power and reactor internals due to its wide service temperature. In the manufacturing process of 316LN steel, the casting blank is usually hot-processed into the finished or semi-finished products. Thus, the hot compressive test is the most common and effective method to simulate the manufacturing processing[1-3]. The 316LN steel is easy to generate fault layer in thermal deformation process due to its low fault energy, but the dislocation climb or cross-slip is difficult to occur. Therefore, in the thermal processing process, the local accumulation of dislocation density is sufficient to cause the dynamic recrystallization (DRX).

Many recrystallization nucleation mechanisms during the high temperature deformation process have been proposed. The grain boundary projection (bow bending) mechanism[4,5] shows that the grain is nucleated by the migration of existing large angle grain boundary under stress. The sub-crystalline coarsening mechanism[6,7] indicates that the grain is nucleated by the rotation of the sub-grains near the grain boundary. The compound twin mechanism[8] indicates that the grain is nucleated by the high mobility interface due to the repeated annealing twinning. These mechanisms may dominate individually or in combination during the DRX process as the important influence factors. In addition, the flow stress is related to the dislocation storage and dynamic recovery (DRV) of the microstructures during the hot deformation. Thus, the constitutive model should contain two elements. Inui et al[9] studied the combination between Voce formalism and improved Kocks-Mecking method to model small strains of flow curves at 700~1000 °C for 316L stainless steel. Angella et al[10] developed a physically-based constitutive model based on the dislocation density theory and DRX kinetics for a

Received date: March 12, 2021
Foundation item: Youth Top Talents Support Project of Shanxi Province (201606); Natural Science Foundation of Shanxi Province (201801D121081); National Natural Science Foundation of China (51474152, 51401143, 51274149)
Corresponding author: Zhao Zhenduo, Ph. D., Professor, State Key Laboratory of Advanced Stainless Steel, Taiyuan Iron and Steel (Group) Co., Ltd, Taiyuan 030003, P. R. China, Tel: 0086-351-2130309, E-mail: zhaozd@tisco.com.cn

nitrogen-alloyed ultralow carbon stainless steel, and the model was of high accuracy for engineering calculation. He et al[11] found that based on the dislocation density theory, the flow stress model can accurately predict the flow curves of stabilized ferrite stainless steel of 12wt%~27wt% Cr. However, the microstructure evolution of 316LN steel has a great impact on the mechanical properties and the hot crack defects occur easily in the hot working process, which brings difficulties to the subsequent processing.

In this research, the high temperature thermal deformation constitutive model of 316LN steel based on the dislocation density theory was established. According to the related fitting curves, the critical strain can be accurately predicted, which is regarded as the threshold for work hardening of DRV and DRX. The thermodynamic behavior of 316LN steel at high temperature under different softening mechanisms and different stages was discussed. The thermodynamic constitutive model based on the dislocation density theory was established.

1 Experiment

The 316LN austenitic stainless steel was prepared in a vacuum induction melting furnace and then cast into ingots, and its chemical composition is 0.012wt% C, 0.50wt% Si, 1.57wt% Mn, 0.015wt% P, 0.001wt% S, 16.62wt% Cr, 13.40wt% Ni, 2.16wt% Mo, 0.15wt% N, and balanced Fe. The ingot was cut by the wire cutting machine into the rectangular specimens with a dimension of 40 mm×80 mm×90 mm after forging at 1200 °C and the cylindrical specimens for thermal simulation with a dimension of Φ10 mm×15 mm. A single hot compression test was conducted using the Gleeble 3800 thermal simulation machine. The specimens were heated to 1200 °C at a heating rate of 10 °C/s and held for 180 s. Then the specimens were cooled to the deformation temperature at the cooling rate of 10 °C /s and held for 10 s to homogenize the microstructures. Then the compressive deformation was conducted. The deformation temperatures were 1050, 1100, 1150, and 1200 °C. The strain rates were 0.1, 1, and 50 s^{-1}. All the specimens were deformed under the engineering strain of 50.34%, i.e., the true strain of 0.7, and then immediately quenched in water to maintain the microstructures.

2 Results and Discussion

2.1 Hot deformation behavior

Fig. 1 shows the true stress-true strain curves of 316LN steels under different deformation conditions. It can be seen that the true stress is increased with increasing the strain rate at the same deformation temperature. The true stress is increased rapidly in the initial stage due to the work hardening effect caused by the generation and propagation of dislocations[12,13].

When the strain rate is 0.1 s^{-1}, the true stress is decreased slightly after reaching the maximum stress and presents a plateau with increasing the true strain, indicating that DRX occurs during this hot compressive deformation[14]. When the strain rate is 1 and 50 s^{-1}, the true stress is increased gradually without an obvious peak stress, as the true strain increases. This phenomenon is in agreement with Ref. [15], indicating that DRV occurs in this hot compressive deformation. In addition, the peak stress of the 316LN steel depends on the temperature and strain rate. With increasing the deformation temperature from 1050 °C to 1200 °C, the peak stress is

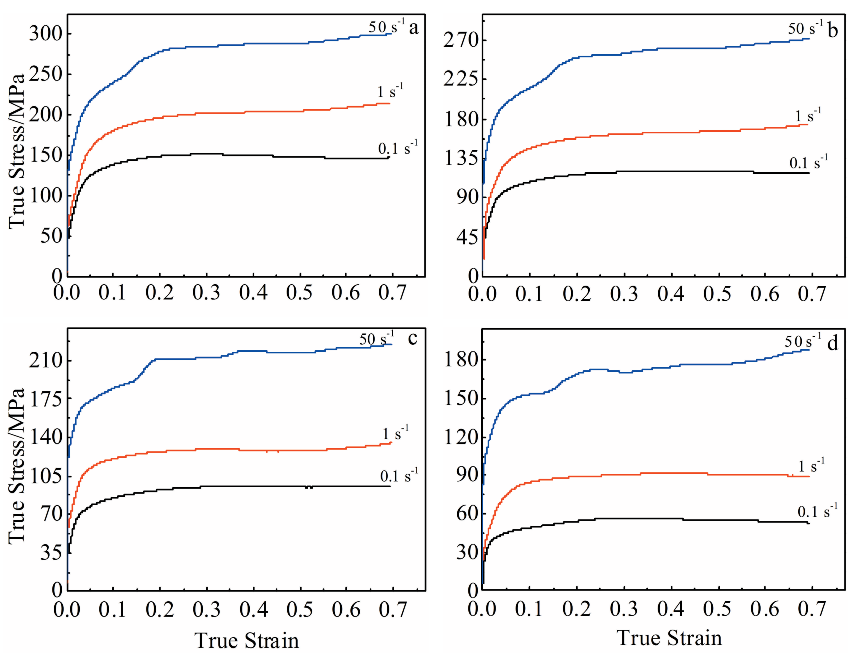

Fig.1 True stress-true strain curves of 316LN steels at different deformation temperatures: (a) 1050 °C, (b) 1100 °C, (c) 1150 °C, and (d) 1200 °C

decreased under a fixed strain rate; with increasing the strain rate, the peak stress is increased under a fixed deformation temperature. The main reasons for this phenomenon are that the kinetic energy of atoms is increased gradually with increasing the deformation temperature and DRX nucleation becomes easier, resulting in a lower peak stress[16]. Whereas under the high strain rate, the time for nucleation or growth of sub-grains is not sufficient, leading to higher peak stress. In addition, under the strain rate of 50 s^{-1} and deformation temperatures of 1050~1200 °C, the true stress-true strain curves show some fluctuations, because the strain rate is very high and the dislocation density increases rapidly, resulting in the rapid increase in stored energy in local area of deformation. Once the stored energy reaches a critical value, the localized recrystallization occurs[17]. After that, the stress becomes stabilized. According to Fig.2b, under the condition of lower strain rate and higher deformation temperature, the peak strain corresponding to the peak stress is smaller.

2.2 Establishment of constitutive model

Two softening mechanisms, DRX and DRV, affect the hot compressive deformation in this research, and Table 1 displays the related process conditions.

2.2.1 DRV-related constitutive model

For metals, both the work hardening and DRV softening

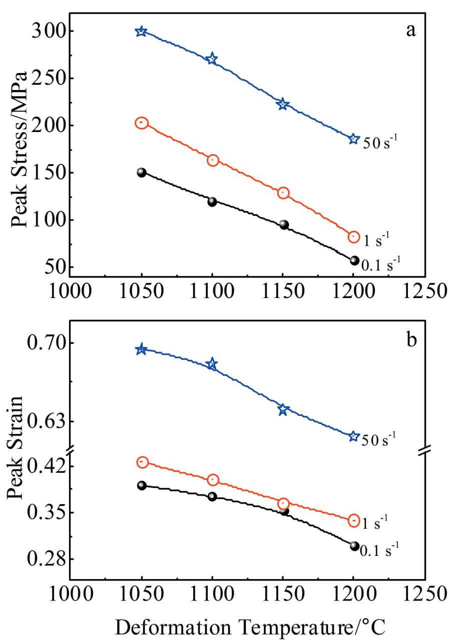

Fig.2 Relationships of peak stress-deformation temperature (a) and peak strain-deformation temperature (b)

Table 1 Hot compressive deformation conditions for different softening mechanisms

Strain rate, $\dot{\varepsilon}$/s^{-1}	Deformation temperature, T/°C	Softening mechanism
$\dot{\varepsilon}\leqslant 0.1$	1050~1200	DRV and DRX
$0.1<\dot{\varepsilon}\leqslant 1$	1200	
$\dot{\varepsilon}>1$	1050~1200	DRV

effects occur during the hot forming process. With increasing the strain, the dislocation density is increased continuously in the work hardening process, whereas decreased in DRV softening process. The dislocation density depends on the competition results of these two processes. According to Pei et al[3], with increasing the strain, the dislocation density can be expressed as follows:

$$\frac{d\rho}{d\varepsilon} = h - r\rho \tag{1}$$

where ρ is the total dislocation density; $\frac{d\rho}{d\varepsilon}$ is the variation of the total dislocation density with strain; h stands for the work hardening strength, representing multiple effects of dislocations; ε is strain; r represents the coefficient of DRV, indicating the probability of annihilation and rearrangement by reactions between mobile and immobile dislocations. Thus, the total dislocation density can be expressed as follows:

$$\rho = \rho_0 e^{-r\varepsilon} + \frac{h}{r}\left[1 - e^{-r\varepsilon}\right] \tag{2}$$

where ρ_0 is the initial dislocation density.

The relationship between the stress and dislocation density during hot compressive deformation can be expressed as follows[18-20]:

$$\sigma = \alpha\mu|\boldsymbol{b}|\sqrt{\rho} \tag{3}$$

$$\sigma_0 = \alpha\mu|\boldsymbol{b}|\sqrt{\rho_0} \tag{4}$$

where σ is the flow stress; σ_0 is the yield stress; α is a material constant; μ is the shear modulus; $\boldsymbol{b}$ is the Burgers vector.

Combining Eq.(2~4), the flow stress in the competition of work hardening and DRV effects can be obtained as follows:

$$\sigma=\left[\sigma_{sat}^2+\left(\sigma_{sat}^2-\sigma_0^2\right)\exp\left(-r\varepsilon\right)\right]^{\frac{1}{2}} \tag{5}$$

where $\sigma_{sat}=\alpha\mu|\boldsymbol{b}|\sqrt{\frac{h}{r}}$ is the flow stress in the steady state, i.e., the softening effect of DRV is balanced with the work hardening effect.

2.2.2 DRX-related constitutive model

With increasing the deformation temperature and decreasing the strain rate, DRX becomes more and more obvious. According to Ref.[21], the flow stress in the steady state after DRX can be expressed as follows:

$$\sigma = F_1 \exp\left[g\left(\varepsilon - \varepsilon_p\right)^2\right] + F_2 \qquad \varepsilon > \varepsilon_c \tag{6}$$

where ε_p is the peak strain, corresponding to the peak stress σ_p; ε_c is the critical strain for DRX occurrence; F_2 is a parameter depending on the steady-state flow stress; when $\varepsilon=\varepsilon_p$, $F_1=\sigma_p-F_2$; g is the material constant of hot deformation.

2.2.3 Determination of critical strain for DRX occurrence

Yanagida et al[22] reported that the critical stress σ_c for DRX is the downward inflection in the lower curve segment of θ ($\theta = \frac{d\sigma}{d\varepsilon}$)-$\sigma$ plot and the critical strain ε_p for DRX is the strain corresponding to σ_c. Ryan et al[23] proposed that the true stress corresponding to the minimum value of $\left|-\left(\frac{\partial\theta}{\partial\sigma}\right)\right|$ on $-\left(\frac{\partial\theta}{\partial\sigma}\right)$-$\sigma$ plot is the critical stress for DRX occurrence, and the critical strain can also be determined by the true stress-true strain curve. Poliak et al[24] found the critical stress and critical strain for DRX occurrence from the inflection point on the θ - σ curve. In order to obtain an accurate critical strain, a sixth-order polynomial is used in this research to fit the σ-ε data, as expressed by Eq.(7):

$$\sigma(\varepsilon) = A_0 + A_1\varepsilon + A_2\varepsilon^2 + A_3\varepsilon^3 + A_4\varepsilon^4 + A_5\varepsilon^5 + A_6\varepsilon^6 \quad (7)$$

where A_0~A_6 are constants under the specific deformation conditions.

Therefore, the work hardening rate θ can be obtained, as follows:

$$\theta = \frac{\mathrm{d}\sigma}{\mathrm{d}\varepsilon} \quad (8)$$

Fig.3 shows the work hardening rate θ-flow stress σ curves under different hot compressive deformation conditions. With decreasing the deformation temperature and increasing the strain rate, the work hardening rate θ of 316LN steel is increased, because θ is determined by the competition between existence and annihilation of dislocations, and DRX and DRV can be mainly neglected under the low deformation temperatures and high strain rates[19]. At low flow stress, θ is decreased rapidly. With increasing the flow stress, θ is decreased slowly. When the flow stress reaches the critical stress σ_c, the dislocation density is increased to the maximum value, and the inflection point appears in the θ-σ curve, indicating the DRX occurrence[19,24-27]. Subsequently, θ decreases rapidly again until to zero, and the peak stress σ_p is obtained.

To identify the critical condition for DRX occurrence, it is necessary to select the reasonable data of critical stress. The true stress-true strain curve obtained under the strain rate of 0.1 s^{-1} and deformation temperature of 1050 °C is used for further analysis of the critical condition for DRX occurrence[13,26].

According to the θ-σ and lnθ-ε curves, the fitting equations

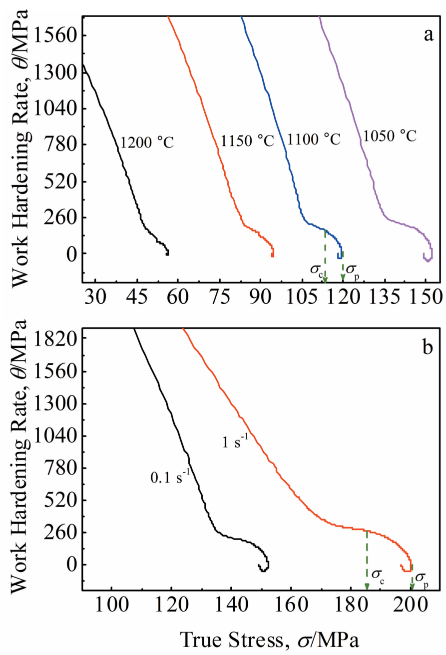

Fig.3 Relationship between work hardening rate θ and flow stress σ under the strain rate of $\dot{\varepsilon}$=0.1 s^{-1} (a) and deformation temperature of T=1050 °C (b)

are expressed as follows:

$$\theta = B_0 + B_1\sigma + B_2\sigma^2 + B_3\sigma^3 \quad (9)$$

$$\ln\theta = B_{01} + B_{11}\varepsilon + B_{21}\varepsilon^2 + B_{31}\varepsilon^3 \quad (10)$$

where B_0~B_3 and B_{01}~B_{31} are constants under the specific deformation condition.

According to Ref.[24,25], there is an inflection point at the critical point of DRX occurrence:

$$\frac{\partial^2\theta}{\partial\sigma^2} = 0 \quad (11)$$

Substituting Eq.(9) into Eq.(11), Eq.(12) can be obtained, as follows:

$$\frac{\partial^2\theta}{\partial\sigma^2} = 2B_2 + 6B_3\sigma_c \quad (12)$$

According to Eq.(11), the critical stress can be obtained, as follows:

$$\sigma_c = -\frac{B_2}{3B_3} \quad (13)$$

The critical strain can also be obtained using the similar calculation, as follows:

$$\varepsilon_c = -\frac{B_{21}}{3B_{31}} \quad (14)$$

The recrystallization critical strain ε_c is not directly obtained through the rheological stress curve, and its value does not correspond to the critical stress σ_c, because the σ-ε curves are fitted by a sixth-order polynomial, resulting in a relatively large deviation of σ_c. As shown in Fig.4, under the strain rate of 0.1 s^{-1} and deformation temperature of 1050 °C, the cubic polynomials fit well with the θ-σ and lnθ-ε curves. Therefore, the fitting results can describe the relationship between work hardening rate and stress/strain. Thus, the critical stress and critical strain under different conditions can be obtained, as shown in Fig.5.

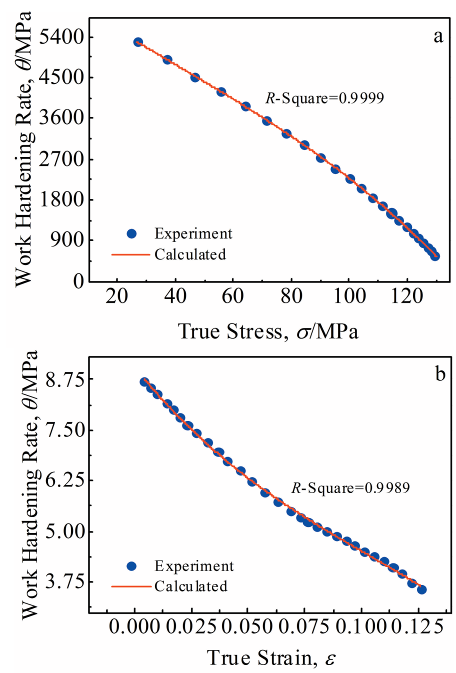

Fig.4 Relationships of θ-σ (a) and lnθ-ε (b) under strain rate of 0.1 s^{-1} and deformation temperature of 1050 °C

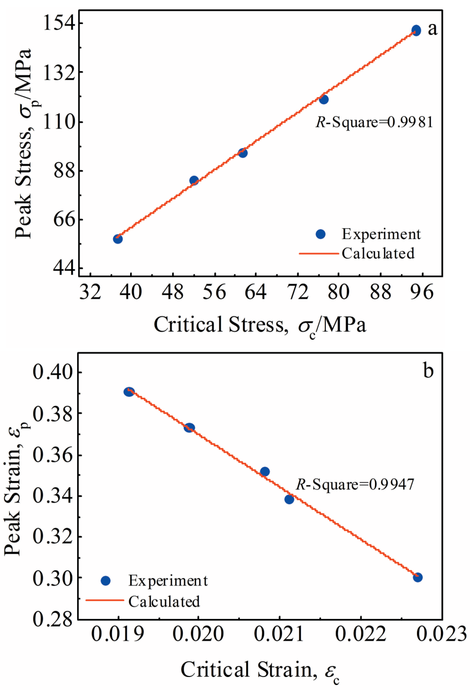

Fig.5 Relationships of σ_p-σ_c (a) and ε_p-ε_c (b) under strain rate of 0.1 s^{-1} and deformation temperature of 1050 °C

When ε_p is small, $\varepsilon_c/\varepsilon_p$ is below the fitting line, i.e., DRX occurs easily under the conditions of low strain rate and high deformation temperature. When ε_p is large, $\varepsilon_c/\varepsilon_p$ is mainly above the fitting line, i.e., DRX is hindered under the conditions of high strain rate and low deformation temperature.

2.2.4 Comprehensive constitutive model

According to the calculation results based on the experiment data of 316LN austenitic stainless steel after single-pass compressive deformation, the related parameters for constitutive model under different conditions can be obtained, as shown in Table 2.

Table 2 Calculated parameters for constitutive model under different deformation conditions

No.	Strain rate/s^{-1}	Deformation temperature/°C	σ_{sat}/MPa	r	F_2/MPa	α
1	0.1	1200	65.78	7.164	46.57	−207.33
2	0.1	1150	113.06	6.862	89.47	−132.52
3	0.1	1100	131.11	6.364	111.91	−93.15
4	0.1	1050	162.24	6.183	140.79	−62.78
5	1	1200	97.68	6.946	85.57	−188.26
6	1	1150	150.09	6.237	-	-
7	1	1100	189.43	5.926	-	-
8	1	1050	227.01	5.913	-	-
9	50	1200	201.09	6.875	-	-
10	50	1150	243.51	5.871	-	-
11	50	1100	283.31	5.497	-	-
12	50	1050	311.24	5.503	-	-

Therefore, the following equations can be obtained:

$$\begin{cases} \sigma_{sat} = P_1\dot{\varepsilon}^{b_1}\exp\left(\dfrac{Q}{RT}\right) \\ r = P_2\dot{\varepsilon}^{b_2}\exp\left(\dfrac{Q}{RT}\right) \\ F_2 = P_3\dot{\varepsilon}^{b_3}\exp\left(\dfrac{Q}{RT}\right) \\ \alpha = P_4\dot{\varepsilon}^{b_4}\exp\left(\dfrac{Q}{RT}\right) \end{cases} \tag{15}$$

where P_1~P_4 and b_1~b_4 are constants; Q is the deformation activation energy; R is the gas constant. The regression calculation of parameters under different deformation conditions was conducted, and the rheological stress models of 316LN austenitic stainless steel at different stages are obtained, as shown in Table 3.

To verify the accuracy of the established constitutive model, the 316LN steels under the condition of 1200 °C/0.07 s^{-1}, 1100 °C/0.05 s^{-1}, 1200 °C/5 s^{-1}, and 1200 °C/25 s^{-1} were selected for comparison. The experiment and calculated stress-strain curves are shown in Fig. 6. It can be seen that the constitutive model can accurately predict the rheological stress.

In order to further verify the constitutive model, the product difference correlation coefficients are introduced, namely, the Pearson simple correlation coefficient r and average absolute relative error (AARE)[28-30]:

$$r = \frac{\sum_{i=1}^{n}\left(E_i - \bar{E}\right)\left(P_i - \bar{P}\right)}{\sqrt{\sum_{i=1}^{n}\left(E_i - \bar{E}\right)^2}\sqrt{\sum_{i=1}^{n}\left(P_i - \bar{P}\right)^2}} \tag{16}$$

Table 3 Constitutive models of 316LN steel under different deformation conditions

Deformation temperature/°C	Strain rate/s^{-1}	Constitutive model
1050~1200	≤0.1	$\begin{cases}\sigma=\left[\sigma_{sat}^2-\left(\sigma_{sat}^2-\sigma_0^2\right)\exp(-r\varepsilon)\right]^{\frac{1}{2}} & (\varepsilon<\varepsilon_c) \\ \sigma=\left(\sigma_p-F_2\right)\exp\left[\alpha\left(\varepsilon-\varepsilon_p\right)^2\right]+F_2 & (\varepsilon>\varepsilon_c)\end{cases}$ with
1200	≤1	$\sigma_{sat} = 7.125\dot{\varepsilon}^{-0.08225}\exp\left(\dfrac{28\,796}{RT}\right)$ $r = 2.404\dot{\varepsilon}^{0.01935}\exp\left(\dfrac{11\,668}{RT}\right)$ $F_2 = 6.925\dot{\varepsilon}^{-0.05528}\exp\left(\dfrac{27\,655}{RT}\right)$ $\alpha=-93.593\dot{\varepsilon}^{4.5968\times10^{-2}}\exp\left(\dfrac{-1.0404\times10^6}{RT}\right)$
1050~1200	>1	$\sigma = \left[\sigma_{sat}^2-\left(\sigma_{sat}^2-\sigma_0^2\right)\exp(-r\varepsilon)\right]^{\frac{1}{2}}$ with $\sigma_{sat} = 9.829\dot{\varepsilon}^{0.08153}\exp\left(\dfrac{32\,508}{RT}\right)$ $r = 1.708\dot{\varepsilon}^{-0.0038}\exp\left(\dfrac{13\,864}{RT}\right)$

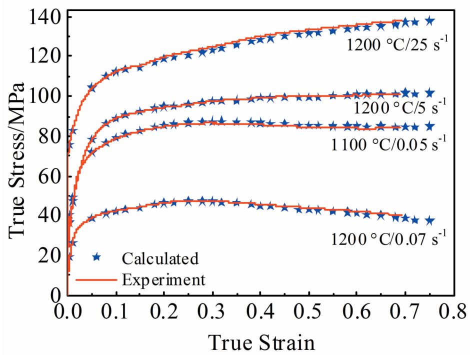

Fig.6 Experiment and calculated true stress-true strain curves under different deformation conditions

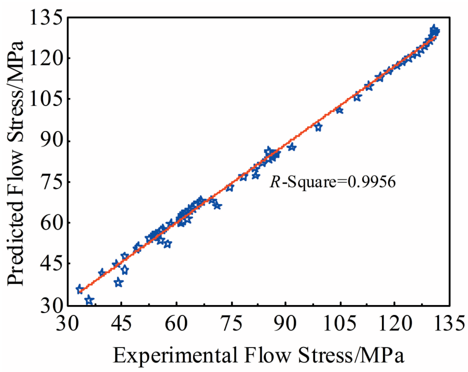

Fig.7 Relationship between calculated rheological stress and experiment stress

$$\mathrm{AARE} = \frac{1}{n}\sum_{i=1}^{n}\frac{\left|E_i - P_i\right|}{E_i} \times 100\% \tag{17}$$

where $\bar{E}$ is the mean value of the experiment value of E_i; $\bar{P}$ is the average value of the calculated value of P_i; n is the number of experiment data.

According to Eq.(16) and Eq.(17), the Pearson correlation coefficient is 0.9956 and the average absolute relative error AARE is 3.07% for predicting the rheological stress. Based on the relationship between the predicted rheological stress and the experiment stress value in Fig. 7, the rheological stress value predicted by the constitutive model is in good agreement with the experiment value with good correlation.

As shown in Fig.7, the established constitutive model based on DRV and DRX can accurately predict the thermal deformation behavior of 316LN austenitic stainless steel under different deformation conditions, providing a reliable theoretical basis for the simulation and practical application.

3 Conclusions

1) The deformation temperature and strain rate have a great influence on the hot compressive deformation behavior of 316LN austenitic stainless steel. The strain is decreased with increasing deformation temperature under the fixed strain rate.

2) The critical stress and critical strain for dynamic recrystallization (DRX) of 316LN steel can be determined by the inflection point of the work hardening rate (θ)-stress (σ) curve and the lnθ-strain (ε) curve. The constitutive model under high temperature deformation is established by regression of related parameters under different deformation conditions.

3) The constitutive model has high accuracy and can precisely predict the rheological stress.

References

1 Pan Pinli, Zhong Yuexian, Ma Qingxian *et al. China Metal Forming Equipment & Manufacturing Technology*[J], 2011, 46(1): 13 (in Chinese)

2 Pei H X, Zhang H L, Wang L X *et al. Materials at High Temperatures*[J], 2014, 31(3): 198

3 Pei Haixiang. *Deformation Behaviors and Mechanism at Different Temperatures of 316LN Stainless Steel for Nuclear Power Plant*[D]. Beijing: University of Science and Technology Beijing, 2015 (in Chinese)

4 Pan Pinli, Zhong Yuexian, Ma Qingxian *et al. J Tsinghua Univ* (*Sci & Tech*)[J], 2013, 53(3): 289 (in Chinese)

5 Huang S H, Hall E L. *Metallurgical Transactions A*[J], 1991, 22(2): 427

6 Dimiduk D, Hazzledine P, Parthasarathy T *et al. Metallurgical and Materials Transactions A*[J], 1998, 29(1): 37

7 Maruyama K, Suzuki G, Kim H Y *et al. Materials Science and Engineering A*[J], 2002, 329-331: 190

8 Montheillet F, Lurdos O, Damamme G. *Acta Materialia*[J], 2009, 57(5): 1602

9 Inui H, Oh M H, Nakamura A *et al. Acta Metallurgica et Materialia*[J], 1992, 40(11): 3095

10 Angella G, Donnini R, Maldini M *et al. Materials Science and Engineering A*[J], 2014, 594: 381

11 He An, Xie Ganlin, Yang Xiaoya *et al. Computational Materials Science*[J], 2015, 98: 64

12 Mehtonen S V, Karjalainen L P, Porter P D. *Materials Science and Engineering A*[J], 2014, 607: 44

13 Li H, Xu M, Li Z T *et al. Ironmaking & Steelmaking*[J], 2017, 45(10): 937

14 Xu Mei, Mi Zhenli, Li Hui *et al. Chinese Journal of Materials Research*[J], 2017, 31(8): 576 (in Chinese)

15 Zhang Wenhui, Sun Shuhua, Zhao Deli *et al. Materials & Design* [J], 2011, 32(8): 4173

16 Liu X G, Ji H P, Guo H *et al. Materials Science and Technology* [J], 2013, 29(1): 24

17 Wang S L, Zhang M X, Wu H C *et al. Materials Characterization*[J], 2016, 118: 92

18 Bergström Y. *Materials Science and Engineering*[J], 1970, 5(4): 193

19 Yoshie A, Fujita T, Fujioka M *et al. Tetsu-to-Hagane*[J], 1994, 80(12): 914

20 Haghdadi N, Martin D, Hodgson P. *Materials & Design*[J],

2016, 106: 420
21 Lin Y C, Chen X M. *Materials & Design*[J], 2011, 32(4): 1733
22 Yanagida A, Liu J S, Yanagimoto J. *Materials Transactions*[J], 2003, 44(11): 2303
23 Ryan N D, McQueen H J. *Canadian Metallurgical Quarterly*[J], 1990, 29(2): 147
24 Poliak E I, Jonas J J. *Acta Materialia*[J], 1996, 44(1): 127
25 Najafizadeh A, Jonas J. *ISIJ International*[J], 2006, 46(11): 1679
26 Toth L S, Molinari A, Estrin Y. *Journal of Engineering Materials and Technology*[J], 2002, 124(1): 71
27 Mecking H, Kocks U F. *Acta Metallurgica*[J], 1981, 29(11): 1865
28 Wang S, Luo J R, Zhang J S *et al*. *Materials & Design*[J], 2016, 107: 277
29 Jia W T, Xu S, Le Q C *et al*. *Materials & Design*[J], 2016, 106: 120
30 Ding Z Y, Hu Q D, Zeng L *et al*. *International Journal of Minerals, Metallurgy, and Materials*[J], 2016, 23(11): 1275

基于位错密度理论的核级316LN不锈钢高温本构模型

赵振铎[1]，李　莎[1]，徐　梅[1]，裴海祥[2]，范光伟[1]，赵子龙[3]

(1. 太原钢铁(集团)有限公司 先进不锈钢材料国家重点实验室，山西 太原 030003)

(2. 中北大学 材料科学与工程学院，山西 太原 030051)

(3. 中山大学 化学工程与技术学院，广东 珠海 519082)

摘　要：研究了316LN奥氏体不锈钢在1050~1200 ℃、应变速率0.1，1和50 s^{-1}下的压缩变形行为，分析了变形温度和应变速率对热流曲线的影响。基于位错密度理论，建立了316LN钢的热变形本构模型，并揭示了316LN钢的软化机理。结果表明，在高温低应变速率（小于0.1 s^{-1}）条件下，动态再结晶（DRX）为主导软化机理；在高温高应变速率（大于1 s^{-1}）条件下，动态回复（DRV）为主导软化机理；在高温及应变速率为0.1和1 s^{-1}条件下，DRV和DRX共同作用。构建的模型可以很好地预测316LN钢的热变形行为，其Pearson相关系数为0.9956，平均相对误差绝对值为3.07%，为一个精确的本构模型。

关键词：奥氏体不锈钢；本构模型；位错密度；软化机制；临界应变；热变形；加工硬化

作者简介：赵振铎，男，1980年生，博士，教授级高工，太原钢铁（集团）有限公司先进不锈钢材料国家重点实验室，山西 太原 030003，电话：0351-2130309，E-mail：zhaozd@tisco.com.cn